Electric Fields and Poynting Fluxes from Vector Magnetograms and Doppler Shifts

George Fisher, Maria Kazachenko, Brian Welsch, and Bill Abbett

Space Sciences Laboratory, UC Berkeley

*For more details, see Kazachenko Poster 26 at SDO4/Hinode/IRIS meeting, and http://arxiv.org/abs/1101.4086 or Solar Physics **277**, p153;* DOI 10.1007/s11207-011-9816-4 (2012)

October 24, 2010 HMI vector magnetic field observations (Thanks to Keiji Hayashi and HMI vector team for movie)

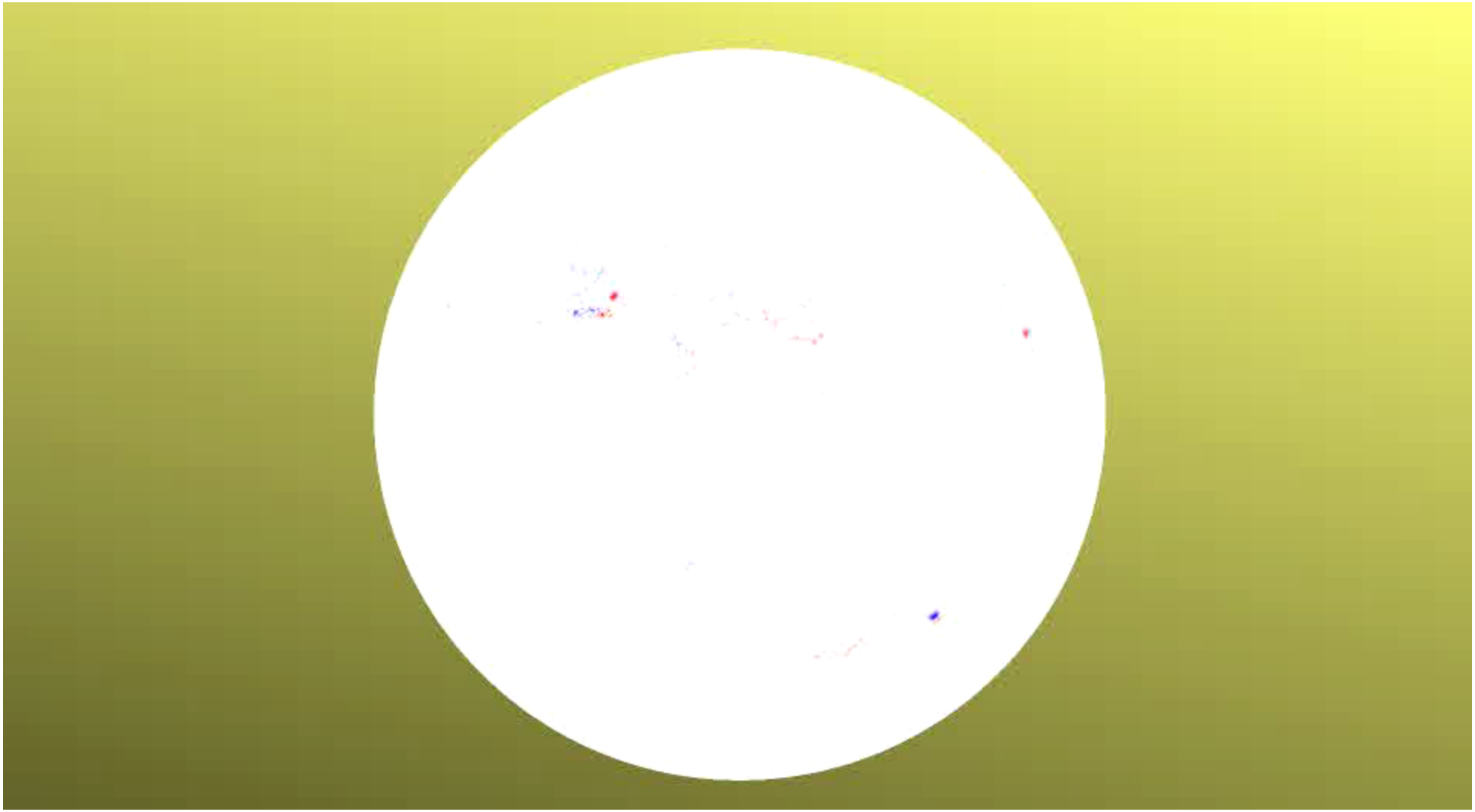

To what extent can we use observations of the evolving magnetic field vector on the photosphere to determine the 3-dimensional velocity field or electric field?

And if you could do this, why would you want to?

If we can determine the electric field from the evolving magnetic field, we can use magnetic evolution observed by HMI to infer the vertical Poynting flux at the photosphere.

$$\mathbf{S} = \frac{1}{4\pi} c\mathbf{E} \times \mathbf{B} \qquad (1)$$

- The electric field **E** appears in the vertical Poynting flux of magnetic energy across the photosphere, and Faraday tells us

$$\frac{\partial \mathbf{B}}{\partial t} = -\nabla \times c\mathbf{E} \; . \qquad (2)$$

Can we invert this equation for **E**?

Since the three-dimensional magnetic field vector is a solenoidal quantity, one can express the magnetic field in terms of two scalar functions, $\mathcal{B}$ (the "poloidal" potential) and $\mathcal{J}$ (the "toroidal" potential), as follows:

$$\mathbf{B} = \nabla \times \nabla \times \mathcal{B}\hat{\mathbf{z}} + \nabla \times \mathcal{J}\hat{\mathbf{z}} \ . \tag{3}$$

Taking the partial time derivative of equation (3) one finds

$$\dot{\mathbf{B}} = \nabla \times \nabla \times \dot{\mathcal{B}}\hat{\mathbf{z}} + \nabla \times \dot{\mathcal{J}}\hat{\mathbf{z}} \ . \tag{4}$$

Here, the overdot denotes a partial time derivative. We will now assume a locally Cartesian coordinate system, in which the directions parallel to the photosphere are denoted with a "horizontal" subscript h, and the vertical direction is denoted with subscript z. One can then re-write equations (3) and (4) in terms of horizontal and vertical derivatives as

$$\mathbf{B} = \nabla_h \left(\frac{\partial \mathcal{B}}{\partial z} \right) + \nabla_h \times \mathcal{J}\hat{\mathbf{z}} - \nabla_h^2 \mathcal{B}\hat{\mathbf{z}}, \tag{5}$$

and

$$\dot{\mathbf{B}} = \nabla_h \left(\frac{\partial \dot{\mathcal{B}}}{\partial z} \right) + \nabla_h \times \dot{\mathcal{J}}\hat{\mathbf{z}} - \nabla_h^2 \dot{\mathcal{B}}\hat{\mathbf{z}}. \tag{6}$$

The z-comp. of (6), the z-comp. of its curl, and its horizontal divergence yield 3 2-d Poisson equations,

$$\nabla_h^2 \dot{\mathcal{B}} = -\dot{B}_z \ , \tag{7}$$

$$\nabla_h^2 \dot{\mathcal{J}} = -(4\pi/c)\dot{J}_z = -\hat{\mathbf{z}} \cdot (\nabla \times \dot{\mathbf{B}}_h), \tag{8}$$

$$\nabla_h^2 (\partial \dot{\mathcal{B}}/\partial z) = \nabla_h \cdot \dot{\mathbf{B}}_h. \tag{9}$$

Eqns. (7)-(9) can be solved using observed data to infer the scalar potentials.

See Fisher et al. 2010 (ApJ 715, 242) for details regarding solution of these equations.

By comparing the form of Equation (2) with Equations (4) and (6) it is clear that the following must be true:

$$\nabla \times c\mathbf{E} = -\nabla \times \nabla \times \dot{\mathcal{B}}\hat{\mathbf{z}} - \nabla \times \dot{\mathcal{J}}\hat{\mathbf{z}} \tag{10}$$

$$= -\nabla_h(\partial\dot{\mathcal{B}}/\partial z) - \nabla_h \times \dot{\mathcal{J}}\hat{\mathbf{z}} + \nabla_h^2\dot{\mathcal{B}}\hat{\mathbf{z}}. \tag{11}$$

Uncurling Equation (10) yields this expression for the electric field $\mathbf{E}$:

$$c\mathbf{E} = -\nabla \times \dot{\mathcal{B}}\hat{\mathbf{z}} - \dot{\mathcal{J}}\hat{\mathbf{z}} - c\nabla\psi \equiv c\mathbf{E}^I - c\nabla\psi. \tag{12}$$

Thus the electric field determined by only using Faraday's Law is not unique. What additional data can we use to determine the non-inductive contributions to the electric field?

Important dynamics is not always apparent in $\Delta \mathbf{B}/\Delta t$ -- e.g., flux emergence!

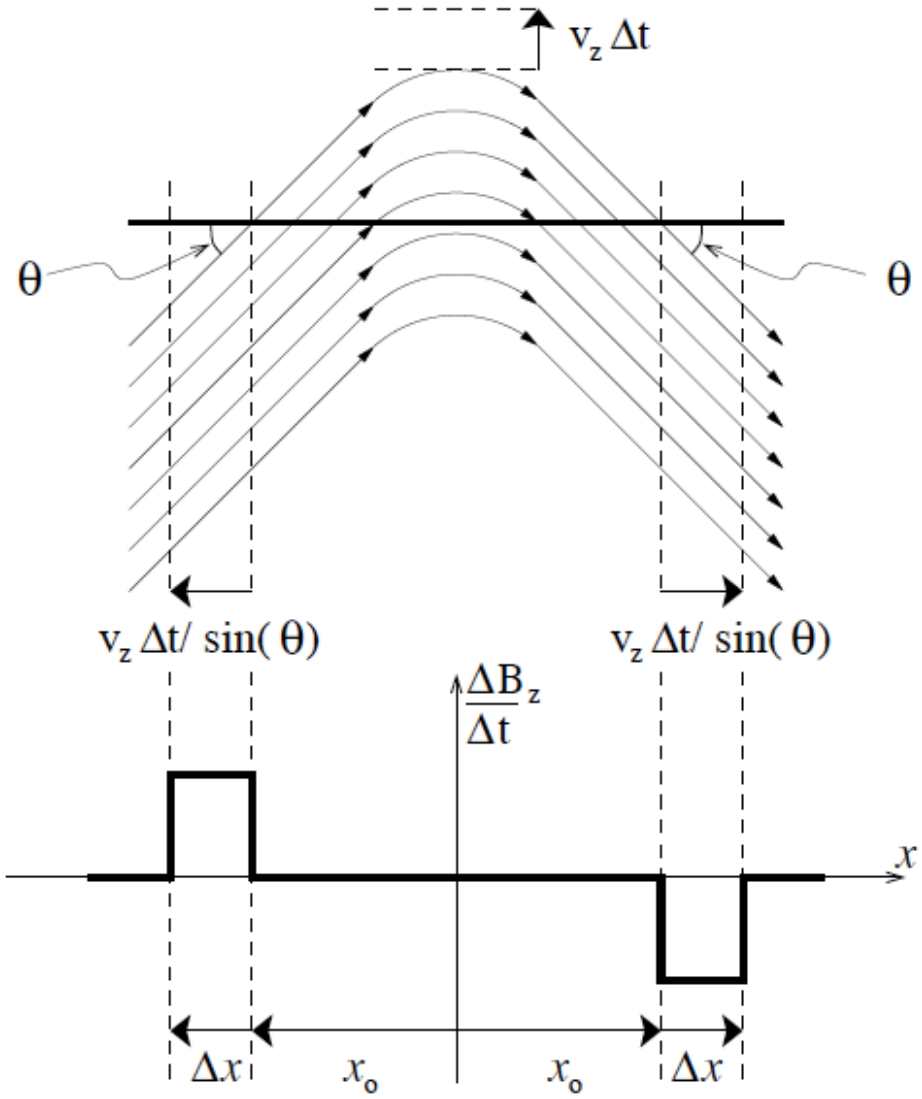

Figure 1. Schematic illustration of flux emergence in a bipolar active region, viewed in cross-section normal to the polarity inversion line (PIL).

The emerging flux is rising at a speed v_z, which could be measured by an observer viewing the active region from above. The length of the bipolar active region (the distance from the edge of one pole to the edge of the other pole) at the time illustrated is $2x_0$.

Note the strong signature of the field change at the edges of the active region, while the field change at the PIL is zero.

What additional information can be used to constrain the inferred electric field **E**? Doppler data!

- Near PILs of the line-of-sight (LOS) field, Doppler shifts and transverse magnetic fields unambiguously determine the "Doppler electric field:"

$$c\mathbf{E}_h^D = -v_z \hat{\mathbf{z}} \times \mathbf{B}_h \ , \qquad (13)$$

- Far away from PILs, flows along **B** (which are unrelated to **E**) contribute to Doppler shifts, so we can't use non-PIL Doppler data

==> Keep PTD solution for $\mathbf{E}'$ in non-PIL regions!

Validation is essential before use with real data! Use MHD simulation with known magnetic field evolution, electric fields, and velocity fields:

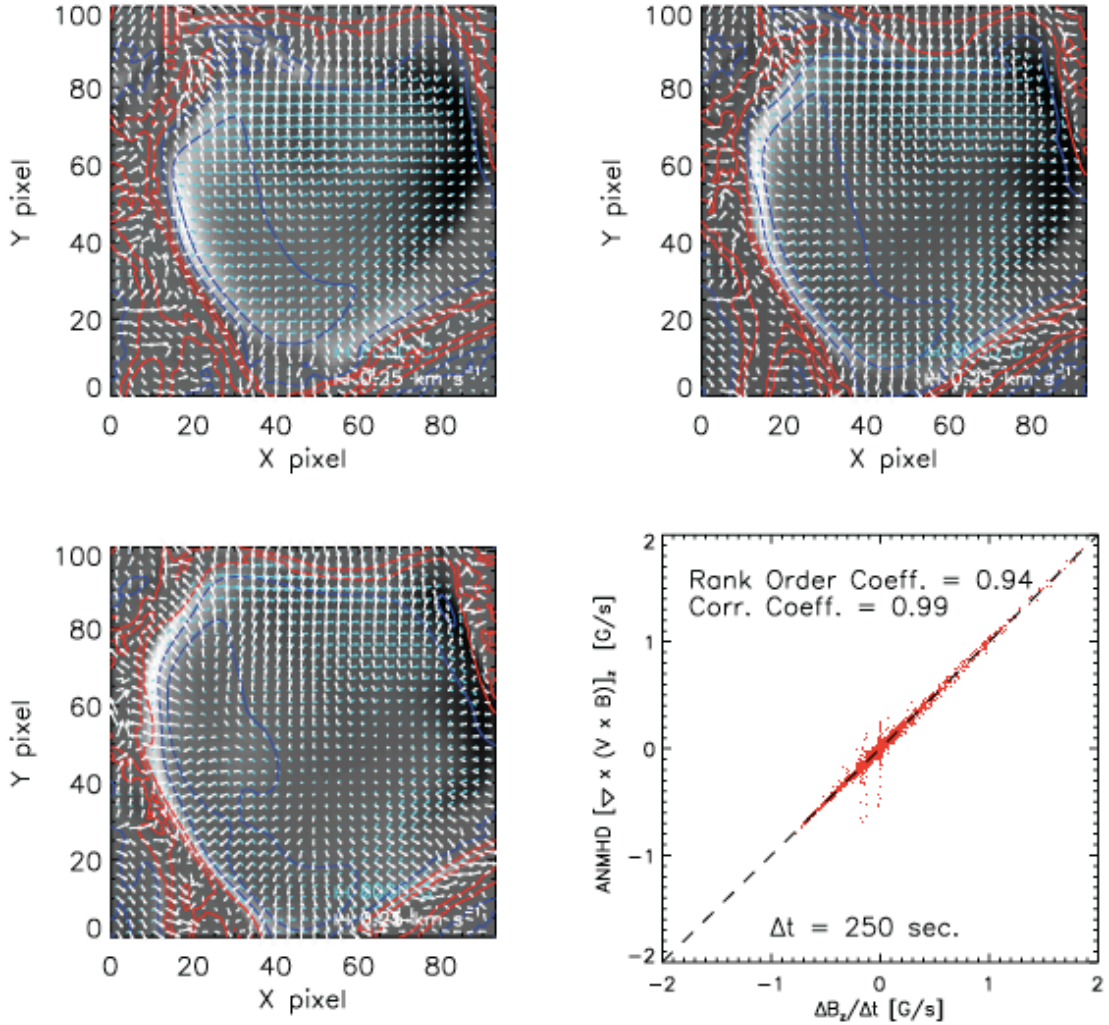

Test case is an ANMHD simulation of a bipolar magnetic region rising through a convecting medium. The simulation was performed by Bill Abbett. Welsch et al. (ApJ 2007) used this same simulation for a detailed evaluation and comparison of velocity/electric-field inversion techniques.

Validation of electric field inversions (test of actual versus inverted vertical Poynting flux and Helicity flux)

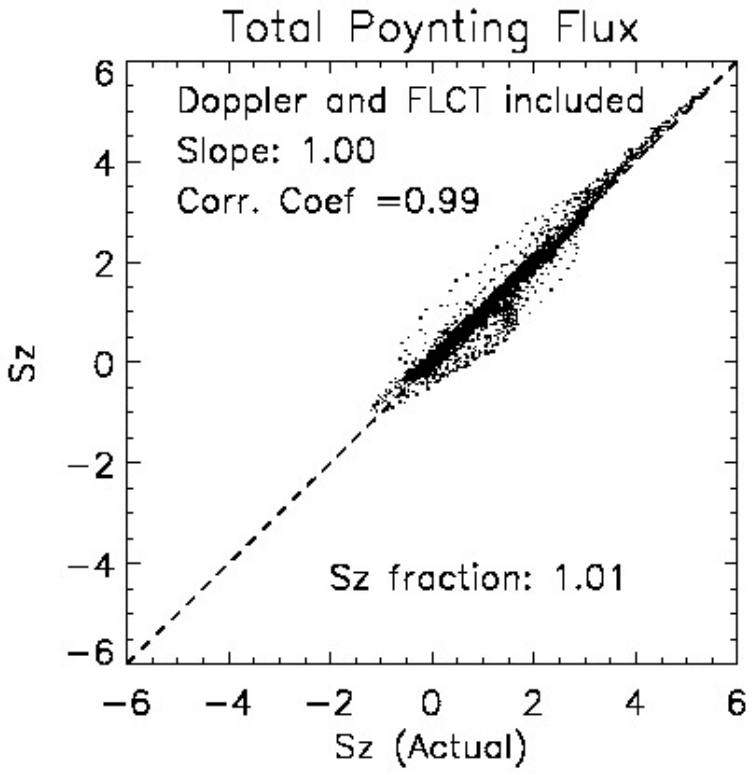

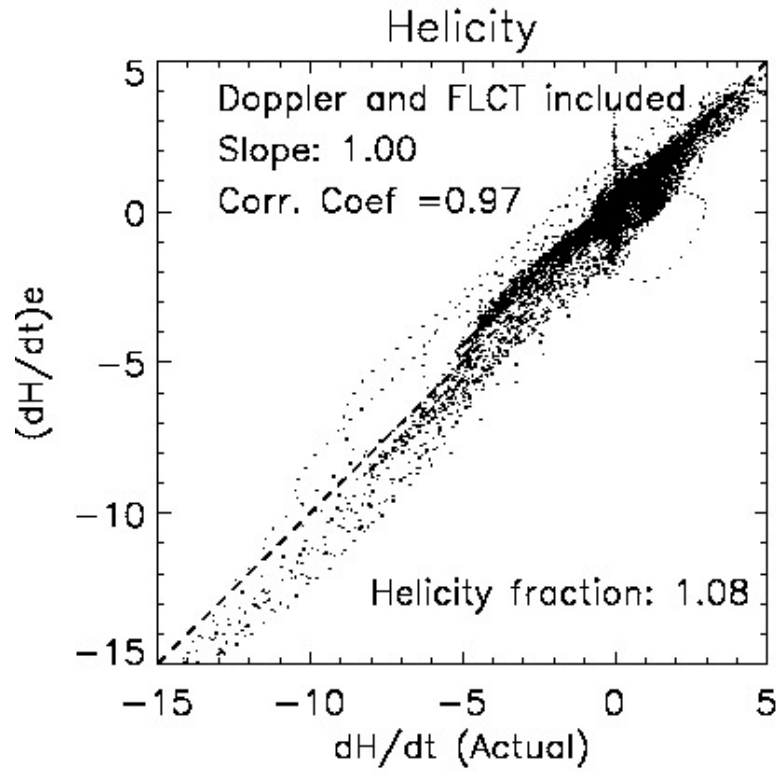

How does the PTD electric field method work away from disk center?

The usage of the $\hat{z}$ vector in the definition of the Poloidal and Toroidal functions can be in *any* direction. In particular, one can choose this vector to point in the line-of-sight direction, with the horizontal directions then residing in the plane-of-the-sky, or "transverse" directions. In this case, the PTD and Doppler Poisson equations can be solved in this coordinate system and then decomposed back into local coordinates on the Sun once the solution is obtained. <u>This is why it is essential to derive all three components of the electric field.</u>

Real world: HMI Observations

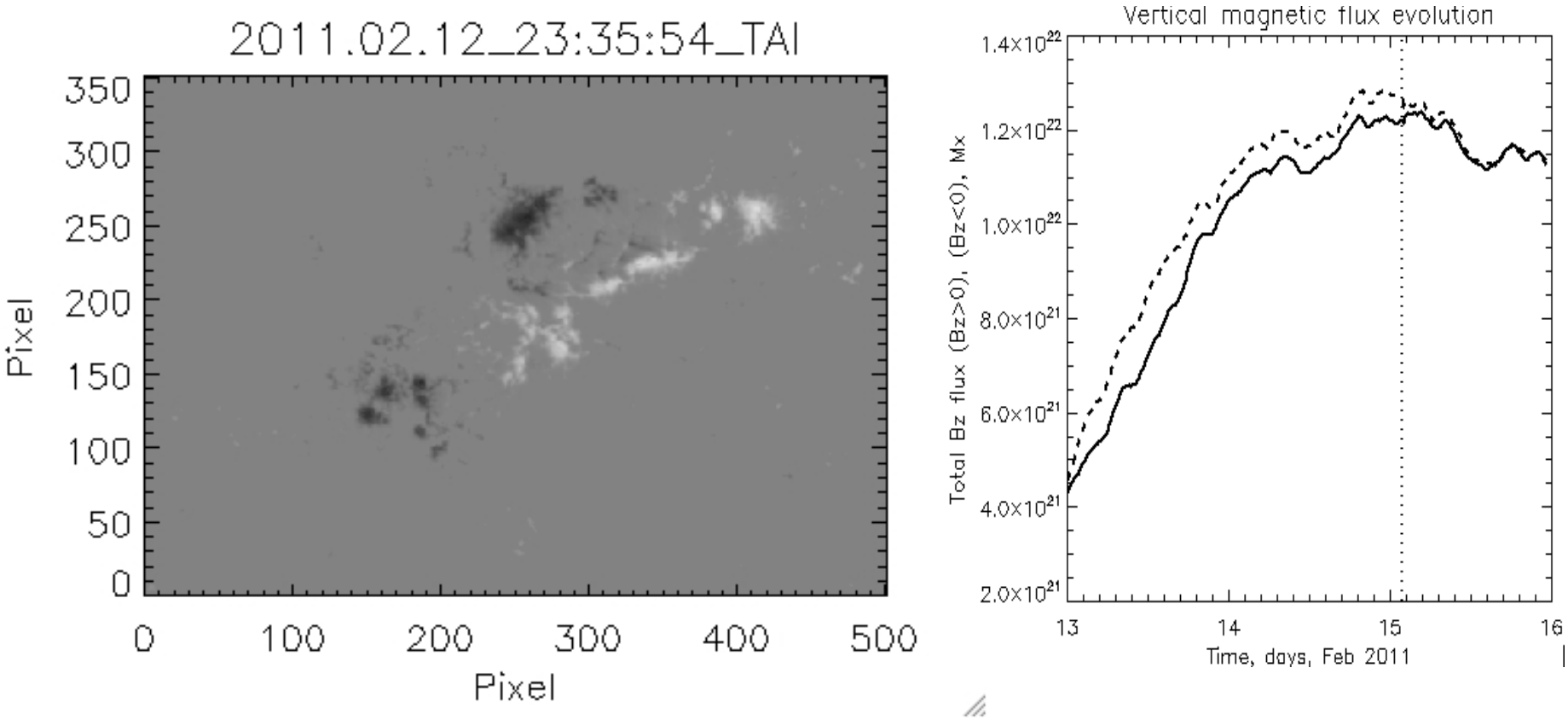

Evolution of Bz in AR 11158: *Left:* Vertical magnetic field Bz observed by HMI, SDO centered on AR 11158 during 3 days of its evolution. *Right:* Solid (dotted) line shows evolution of total positive (negative) vertical magnetic flux from Feb 13 00:00 UT to Feb 15 00:00 UT 2011. The vertical dotted line shows the X2.2 flare peak time: 01:56 UT Feb 15.

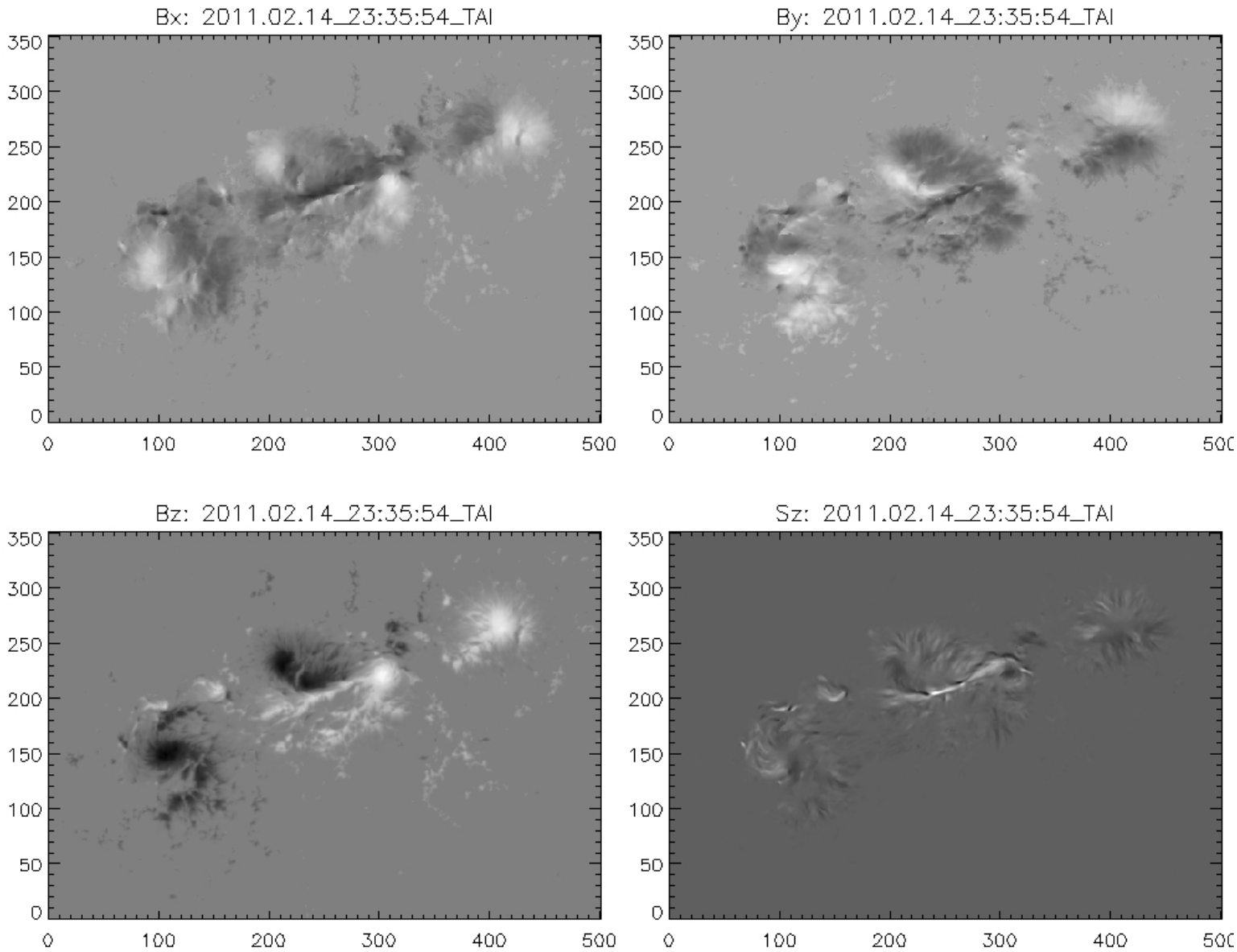

Evolution of Bx, By, Bz, Sz in AR 11158 around flare time: *Top Left:* Bx; *Top Right:* By; *Bottom Left:* Bz. *Bottom Right:* Total Vertical Poynting flux Sz from 23:35 UT Feb 14 to 05:35 UT Feb 15. The X2.2 flare peaks at 01:56 UT on Feb 15 2011.

Decomposition of total Poynting flux into the flux of free energy and the flux of potential-field energy:

$$S_z = \frac{c}{4\pi}(E_x B_y - E_y B_x) = \frac{c}{4\pi}\left[E_x\left(\frac{\partial J}{\partial x} - \frac{\partial}{\partial y}\frac{\partial \beta}{\partial z}\right) - E_y\left(-\frac{\partial J}{\partial y} - \frac{\partial}{\partial x}\frac{\partial \beta}{\partial z}\right)\right] =$$

$$\underbrace{\frac{c}{4\pi}\left(E_x \frac{\partial J}{\partial x} + E_y \frac{\partial J}{\partial y}\right)}_{S_{zfree}} + \underbrace{\frac{c}{4\pi}\left(-E_x \frac{\partial}{\partial y}\frac{\partial \beta}{\partial z} + E_y \frac{\partial}{\partial x}\frac{\partial \beta}{\partial z}\right)}_{S_{pot}}$$

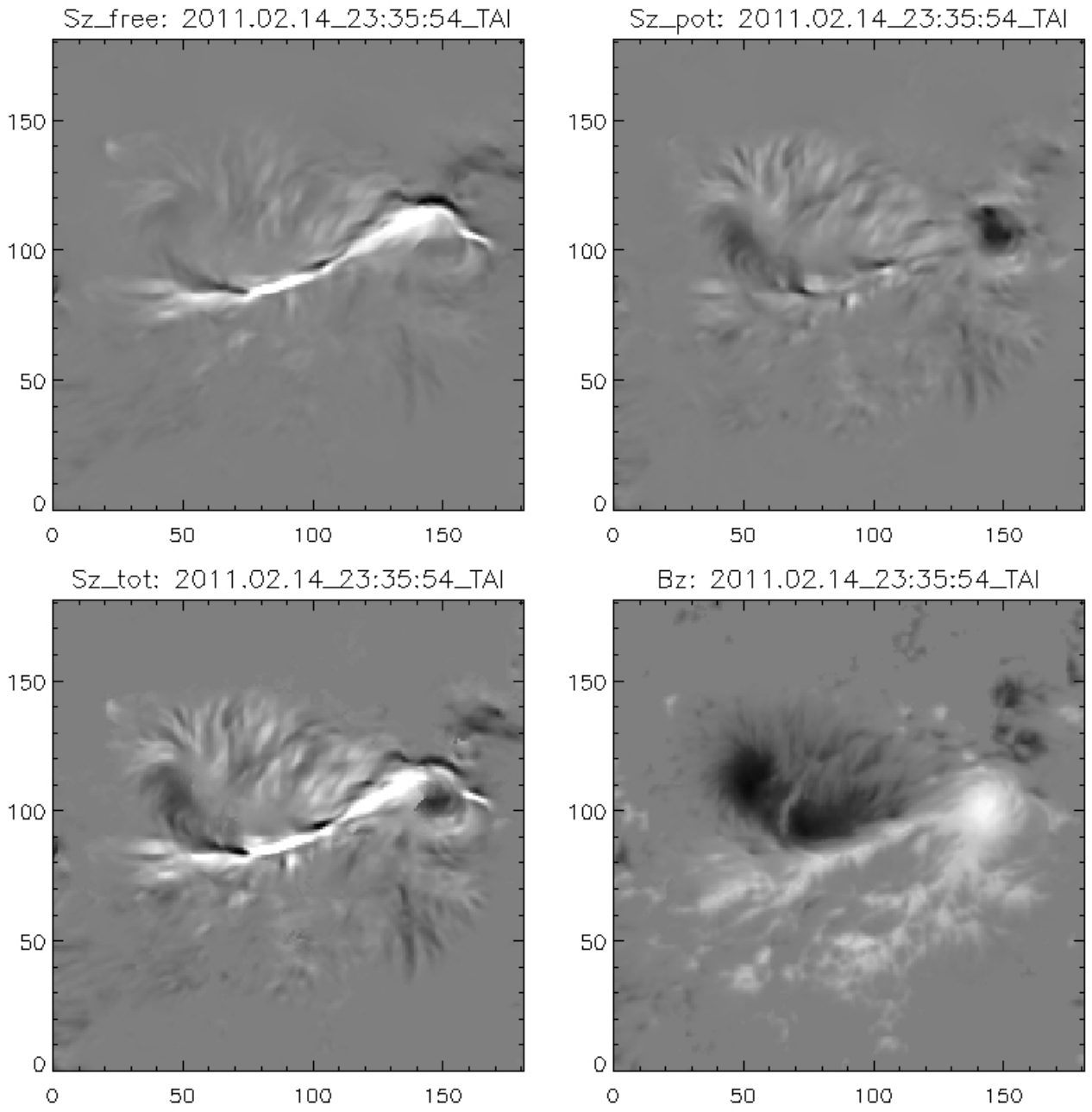

Evolution of Sz components around flare time: *Two top panels:* Two parts of the vertical Poynting flux: the flux of free magnetic energy and the flux of potential-field energy. *Bottom Left:* The sum of the two parts, i.e. the total vertical Poynting flux; *Bottom Right:* Vertical magnetic field Bz observed by HMI. White (black) shows positive (negative) values. All plots are for time period from 23:35 UT Feb 14 to 05:35 UT Feb 15. The X2.2 flare peaks at 01:56 UT on Feb 15 2011.

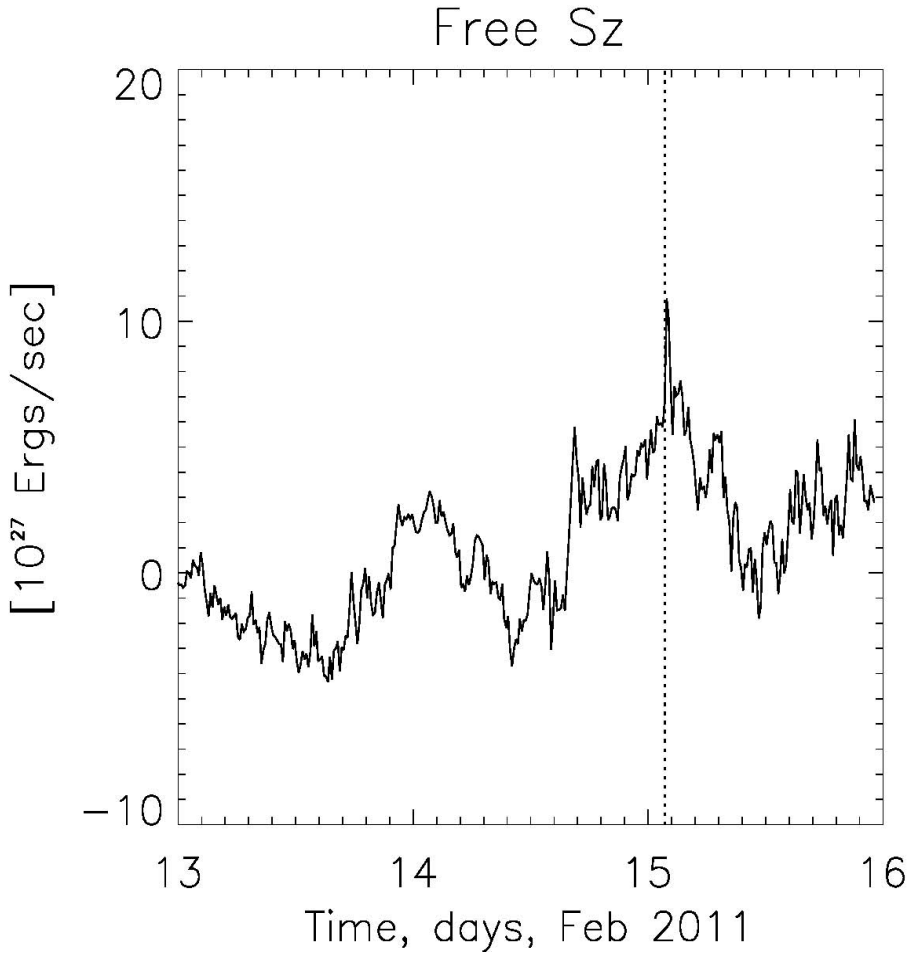

Free energy: Area-integrated free-energy component of the Poynting flux.

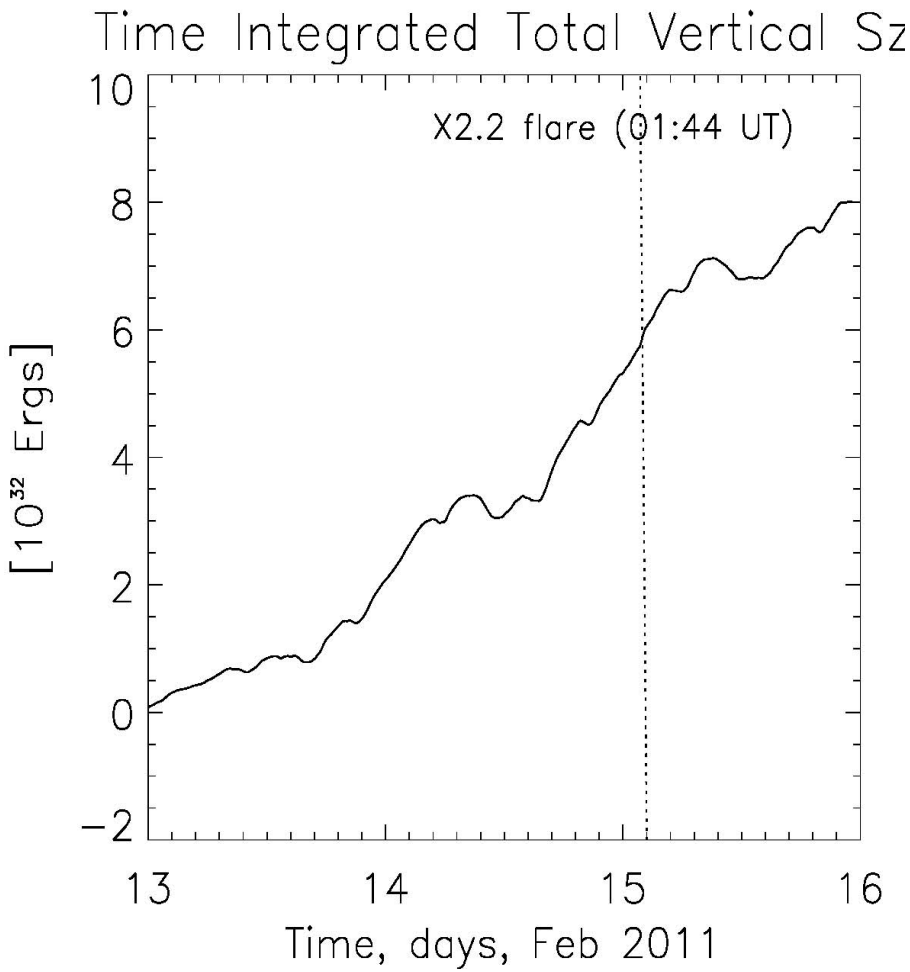

Total Vertical Poynting Flux: Time evolution of area- and time-integrated total vertical Poynting flux in AR 11158. The vertical dotted line shows the flare start time, at 01:44 UT.

What next?

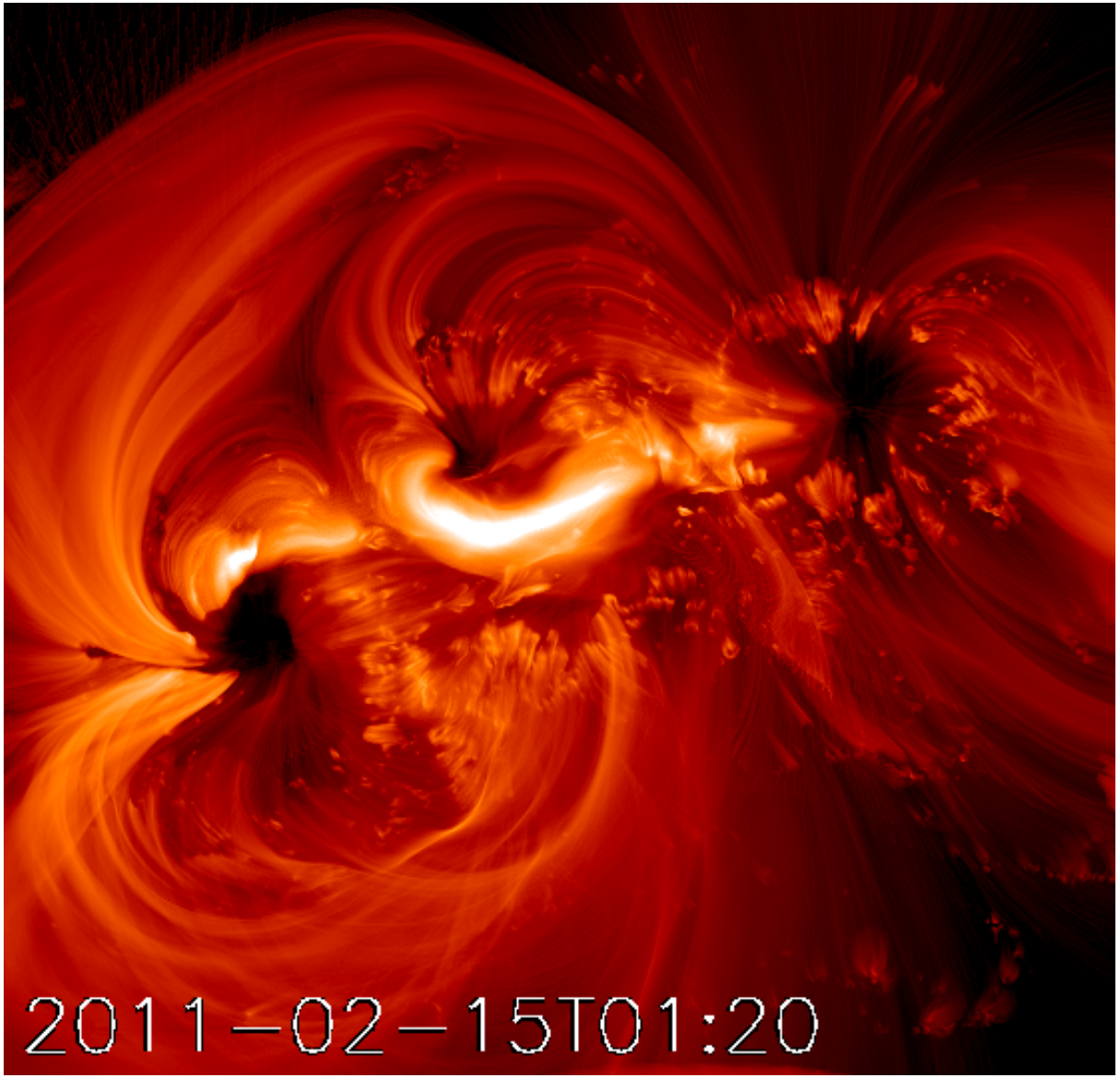

Use the electric fields to drive a coronal magnetic field simulation. The electric fields we derived from AR 11158 were used to drive a magnetofrictional model of the corona above the active region, over a period of 3-days. The coronal configuration was initially potential, but currents build up, and a magnetic eruption occurred at the time of an observed X2.2 flare on Feb. 15, 2011. The simulation was carried out by Mark Cheung of LMSAL. See yesterday's eposter by Cheung.